INDIAN JOURNAL OF SCIENCE AND TECHNOLOGY

*Corresponding author.

kanishka.acc.cs@gmail.com

Brain MRI/CT Contrast Enhancement using Hybrid Transformation

Tanmoy Kanti Halder[1], Kanishka Sarkar[2]*, Ardhendu Mandal[3], Bikramadittya Bagchi[4]

1 Assistant Professor, Computer Science, Prasannadeb Women's College, India
2 Assistant Professor, Computer Science, Ananda Chandra College, India
3 Associate Professor, Computer Science and Engineering, University of North Bengal, India
4 Assistant Teacher, Computer Science, Techno India Group Public School, Hill Cart Road, Darjeeling, India

Abstract

Objectives: To develop a better method for enhancing head MRI or CT images with the objective of suppressing irrelevant information during subsequent processing. **Methods:** To achieve this, two innovative image enhancement techniques, 'AHE' and 'Adaptive Gamma with CDF-based Geometric Transformation,' are combined. The proposed method is evaluated using a total of 76 MRI and 137 CT scan images obtained from the TCIA, OASIS, BCIIHM, and Brain metastases datasets. To tailor these methods for head MRI and CT images, two background masking algorithms have been introduced in this regard. Furthermore, the dark, grey, and white segments of the histogram are identified and geometrically transformed into square areas, followed by a gamma transformation applied to each transformed segment. Finally, a combination of global gamma transformation and AHE is applied to achieve the final enhancement. The proposed method is compared with other state-of-the-art techniques based on evaluation parameters such as "contrast, "correlation, and "entropy. **Findings:** Both qualitative and quantitative analysis exhibit how the proposed method has better enhancement capability than the CLAHE, AGC, and EGC methods. Our approach yields the highest average contrast, correlation, and entropy values for MRI, measuring 0.522319529, 0.957321634, and 5.585280467, respectively. For CT images, the suggested approach produces the maximum entropy value, 3.472600537, and the average contrast, 0.151943828, which is just less than CLAHE. The average correlation for CT, 0.98799312, is also a hair less than EGC. These results suggest that the proposed method could potentially make the details and structures in the MRI and CT more distinguishable. **Novelty :** The suggested approach uses a 2D geometric transformation for enhancing contrast of brain CT/MRI images and two robust head masking processes for removing noise in the background. The comparative analysis shows that the proposed method exhibits superior contrast enhancement capability compared to the other three methods being compared.

1 Introduction

Contrast enhancement methods for general images are not always constructive for medical images. Figure 1(a) shows a low contrast brain MRI image, and Figure 1(b) shows the contrast-enhanced image using general histogram equalization operation. It is worth noting that medical images often contain a plain background, and the presence of noise in the background significantly affects the enhancement process, as depicted in Figure 1.
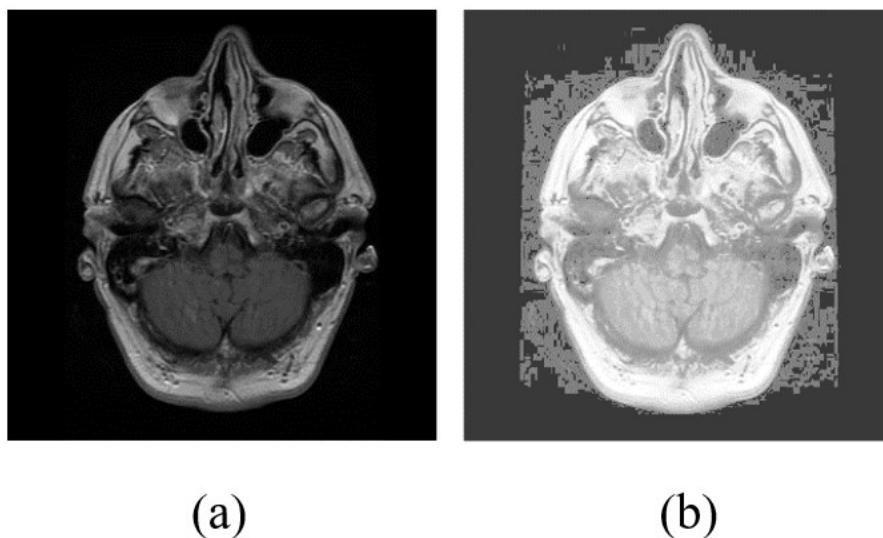

Fig 1. (a) A low contrast brain MRI image (b) Contrast Enhancement using Histogram Equalization

In the past two decades, numerous concepts of histogram processing have been extensively explored for contrast enhancement in medical images[1]. Sakshi Patel et al[2] conducted experiments involving various histogram-based approaches for contrast enhancement. They compared the effectiveness of typical Histogram Equalization (HE), Local Histogram Equalization (LHE), Brightness Preserving Bi-Histogram Equalization (BBHE), Dualistic Sub-Image Histogram Equalization (DSIHE), and Recursive Sub-image Histogram Equalization (RSIHE). The results of their study indicate that DSIHE and RSIHE exhibit superior enhancement capability compared to the other three methods. C. Rubini et al, in their work[3], have experimented Contrast Limited Adaptive Histogram Equalization (CLAHE) and Adaptive Histogram Equalization (AHE) for MRI enhancement. However, in regions with a relatively uniform background, AHE tends to amplify noise because it treats all pixels equally and doesn't differentiate between noise and meaningful image details. This problem is somewhat solved by CLAHE.

Besides Histogram-equalizations, Gamma transformation also provides a significant contribution to contrast enhancement. Somasundaram Karuppanagounder[4] proposes an Empirical gamma transformation method. Here, gamma has been computed from the minimum, maximum, and median intensity, as shown in Equation-1 and Equation-2.

$$\gamma = log\left(\frac{median - minimum}{maximum - median}\right) \qquad (1)$$

$$\gamma = \begin{cases} 0.8 & \text{if } \gamma < 0.8 \\ 1.2 & \text{if } \gamma > 1.2 \\ \gamma & \text{Otherwise} \end{cases} \qquad (2)$$

Mouna Sahnoun et al.[5] proposed an adaptive gamma correction method for enhancing MRI images, in which four distinct image classes are defined based on contrast and brightness levels. Empirical values are then employed to calculate the gamma (γ) value. Ravi Kumar et al.[6] introduced an adaptive weighted distribution-oriented gamma correction method specifically designed for brightness correction and modification of MRI images. In a separate study, Agus Zainal Arifin et al.[7] utilized gamma correction for teeth image segmentation. They conducted experiments with gamma values ranging from 1 to 10.

On the other hand, A. Vijaya Lakshmi et al.[8] recently proposed an MRI enhancement approach based on image regularizations. Although the results of this approach were promising, the enhancement parameters had to be set manually. In another study[9], researchers experimented with the combination of Singular Value Decomposition (SVD) and Discrete Wavelet Transformation (DWT) to enhance the contrast of medical images.

In the past two or three years, researchers have increasingly utilized Convolutional Neural Networks (CNN) for this purpose. Pooja Patel[10] proposed a block-based CNN architecture in which the input image is divided into 32x32 blocks. Each block is then enhanced using the CNN based on a loss function. Similarly, Chao Chen[9] employed a CNN architecture to generate a comparable image to T1 with gadolinium contrast (T1C) using T1, T2, and Apparent Diffusion Coefficient (ADC) images. One significant limitation of utilizing machine learning or deep learning approaches is the availability of datasets. Training complex networks requires a substantial number of images, which can be time-consuming.

In the context of head MRI or CT images, the background often consists of a dark homogeneous region. This study explores the use of Adaptive Histogram Equalization (AHE) and a power law transformation technique to enhance the contrast of the head object in these images.

While AHE and power law transformation are commonly used methods for contrast enhancement, but they were not satisfactory for enhancing the contrast of the head object in the presence of a dark homogeneous background. Instead, these methods might have amplified the background noise, leading to undesirable outcomes.

To address this limitation, the study has tuned and combined the AHE and power law transformation techniques to achieve better contrast enhancement specifically for head MRI or CT images. By adapting these methods and potentially introducing modifications, the study aims to improve the contrast of the head object while minimizing the amplification of background noise.

2 Methodology

In this study, we combine Adaptive Histogram Equalization with a recent gamma correction-based contrast-enhanced method[11] to enhance brain MRI and CT images. Additionally, the presence of irrelevant information in the background of head medical images can lead to undesirable outcomes in subsequent processing steps. This research introduces two novel approaches that utilize histogram processing exclusively to generate a reference mask image for background removal.

The proposed method eliminates the need for manual setting of enhancement parameters. The innovative background masking process guarantees that background noise has no impact on head object enhancement. Additionally, unlike machine or deep learning methods, the proposed method does not require any training dataset.

The study was conducted using a total of 76 MRI and 137 CT scan images. The MRI images were obtained from two different datasets: 15 MRI images from the TCIA[12] dataset and 61 images from disc 1 of the OASIS dataset[13]. On the other hand, 15 CT scan images with relatively low contrast were selected from the "Brain CT Images with Intracranial Hemorrhage Masks (BCIIHM)" dataset[14,15] and 122 images were downloaded from the "Brain metastases" dataset[16]. A comparison with other methods was performed using these 213 head images, evaluating contrast, correlation, and entropy.

The proposed method performs MRI/CT image enhancement in two phases: removing the background pixels in the initial phase and incorporating the brain histogram in the subsequent phase.

Next, the "Adaptive Power-law and CDF-based Geometric Transformation for Low Contrast Image Enhancement"[11] and Adaptive Histogram Equalization have been utilized for enhancement purposes. Figure 2 illustrates an overview of the workflow, and the detailed procedure will be explained in the subsequent sections.
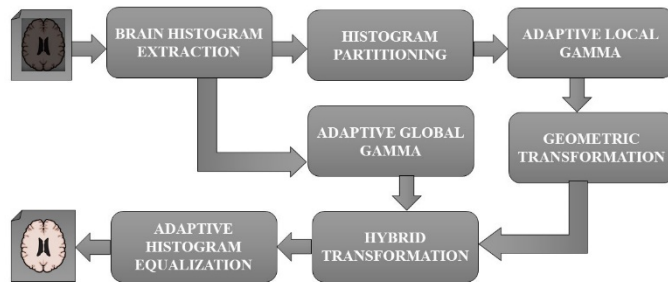
Fig 2. Work flow of the proposed method

2.1 Background Masking

Before actual enhancement is applied, a reference mask image is generated to isolate the brain object from the image. The backgrounds of medical images are considered insignificant and can lead to undesirable outcomes in further processing. Otsu's threshold method[17] has been utilized in most articles to remove plain background noises. However, this method fails for images with irregular boundaries and non-homogeneous background noises (Figure-5a, 5e). In this regard, a better result may be produced by employing an adaptive threshold that discriminates between the actual background and intra-dark intensities of the brain. Two different methods for head masking have been experimented with, and these two methods are discussed below.

2.1.1 Euclidean Distance-based Mask

In the background of MRI images, there exist numerous dark pixels, which are represented as the tallest bin (T_b) in the histogram H (Figure 3). The intention of the proposed method is to locate the fold point (Figure 3) of the background peak and normalize the peaks of the histogram ($H_{normalized}$) to the range of 0 to 255, using Equation-3.

$$H_{normalized} = \frac{H \times (255 - Min(H))}{Max(H)} + Min(H) \tag{3}$$

Then, the Euclidean distance (D_i) (Equation-4) from the bottom (considering $count_b = 0$) of the background peak (T_b) to other bins (i) is computed.

$$D_i = \sqrt{(i - T_b)^2 - (count_i)^2} \tag{4}$$

Equation-5 finds the minimum distance providing intensity, hence considered as the masking threshold 'T'.

$$T = \underset{i}{argmin} D_i \tag{5}$$

Finally, the largest-connected component has been extracted from the binary image, and the hole filling operation is applied to obtain the final mask. Then, the final mask image is multiplied by the original image to extract the brain portion. Subsequently, the brain histogram is stretched using Equation-6.

$$I(u,v) = \frac{I(u,v) - I_{min}}{I_{min} - I_{max}} \tag{6}$$

where I_{max} and I_{min} is the maximum and minimum intensity of the original input image.

Next, the histogram of the image is obtained, and the count of '0 − intensity' is removed to keep out the background for further processing.
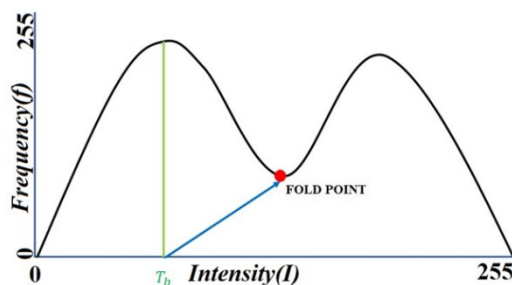
Fig 3. Least Centre Distance Threshold

2.1.2 *Double Otsu's Threshold*

The traditional Otsu's threshold method is considered to include many parts of a head-scan object as a background. Consequently, for an edge-blurred head MRI/CT image, the full mask image cannot be restored through the hole filling operation. To address this situation, the distinction between dark background intensities and intra-head component pixels is achieved by recomputing the Otsu's threshold in the lower portion of the histogram. The computation of the Double Otsu threshold in comparison to the Original Otsu's method is shown in Figure 4. Additionally, Figure 5 illustrates the mask images obtained from the Otsu's threshold method, adaptive threshold, and the proposed methods.

2.2 Adaptive local gamma computation

In this phase, the brain histogram is partitioned into three homogeneous sections by computing the fold points between the three phases. The process of selecting the fold points has already been discussed in the 'Initial Mask generation' section. The computation of the adaptive local γ is performed using Equation-7.

$$\gamma_x = \frac{-1}{ln(r_{mean})} \tag{7}$$

where r_{mean} is the relative mean of partition x, ranging between 0 and 1.
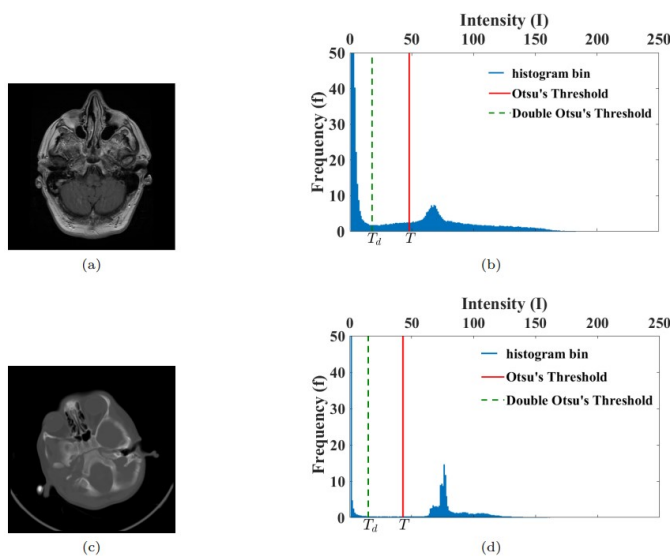

Fig 4. Double Otsu Threshold : (a) An MRI sample image (b) Double otsu threshold computation of Figure4a (c) A CT sample image (d) Double otsu threshold computation of Figure-4c
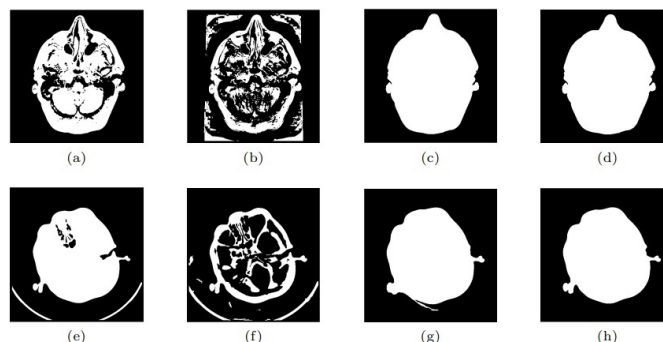
Fig 5. Mask (a-e) Generated by the Otsu's threshold method (b-f) Adaptive threshold (c-g) Euclidean Distance-based method (d-h) Double Otsu threshold method

2.3 Local gamma and CDF-based geometric transformation

The intensities of local sections need to be transformed according to the sectional CDF, and thus a hypothetical square transforming window is assumed by computing the diagonal D_x. In this regard, the sectional CDF is computed for each partition. Furthermore, a contrast factor (CF) is evaluated from the sectional mean using Equations 8 and 9.

$$Mean_x = \frac{\sum_{i=s_x}^{e_x} i \times n_i}{\sum_{i=s_x}^{e_x} n_i} \tag{8}$$

where, s_x and e_x denotes starting and ending intensity of partition x correspondingly ranging between 0 and 1, and n_i represents the pixel count of intensity i.

$$CF = Mean_{First} - Mean_{Last} \tag{9}$$

Next, the Sectional CDFs are adjusted based on the contrast factor (CF) using Equation-10.

$$CDF_x' = CDF_x * (1 - CF) + l_x * CF \tag{10}$$

where, l_x is the length of section x, defined as:

$l_x = e_x - s_x$

Then, the diagonal of the hypothetical square transforming window is computed using Equation-11.

$$D_x = \sqrt{\frac{\left(CDF_x'^2 + l_x^2\right)}{2}} \tag{11}$$

where, l_x is the length of the section.

Hence, gamma transformation is applied for each D_x, where the hypothetical square transforming window is geometrically transformed to the actual transforming window through scaling and translation. This concept has been graphically illustrated in Figure 6.

2.4 Global gamma transformation and Adaptive Histogram Equalization

A global gamma transformation is applied to the entire histogram to maintain consistency among the sections. Hence, the average transformation is obtained from the global and local gamma. Unlike the local gamma, the global transformation is computed using the global mean (Equation-12).

$$\gamma_g = \frac{-1}{ln\left(Mean_g\right)} \tag{12}$$

where, $Mean_g$ is the global mean of the brain.

Later, a combined transformation matrix is obtained from the local gamma and global gamma transformation matrices. Following that, the input image is subjected to gamma transformation. Finally, the gamma-transformed image is equalized using Adaptive histogram equalization.
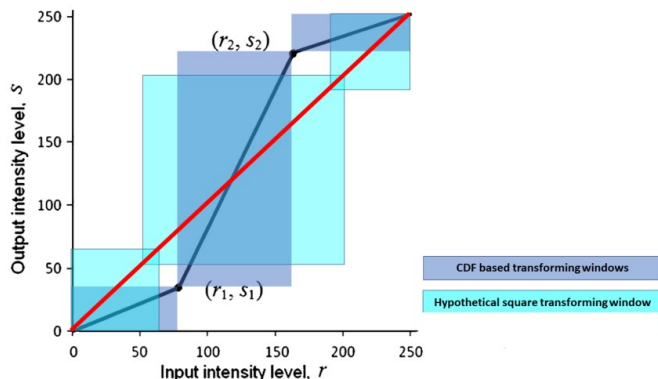
Fig 6. CDF-based Geometric Transformation

3 Results and Discussion

The proposed method for medical image contrast enhancement has been compared with CLAHE[3], AGC[5], and the method of S. Karuppanagounder et al.[4].

3.1. Qualitative Assessment

3.1.1 MRI

Due to space constraints, the qualitative assessment was conducted with 5 sample images. Figure-7 displays the comparative visual outputs, where the first row showcases the five sample images. The second row represents the respective outputs of the gamma transformation method suggested by S. Karuppanagounder et al.[4]. The third row illustrates the outputs of Adaptive gamma Correction proposed by[5], and the fourth row displays the outputs of CLAHE. The last row exhibits the output of the proposed hybrid transformation. Since both proposed head masking procedures generate identical masks for MRI images, the outputs are the same for both the proposed approach, and the common output is shown in one row (last row).

The gamma transformation method of S. Karuppanagounder et al.[4] results in an overall increase in brightness of the input images. However, the AGC method[5] transforms CSF intensities into lower values, leading to degraded visual clarity. On the other hand, a slight amplification of CSF intensity is observed for CLAHE. Furthermore, soft edges of the CSF structure are also maintained to some extent in this case.

The two previously discussed mask generation processes produce nearly identical masks for the reference MRI images, resulting in no visual difference among the corresponding outputs. Regardless of the mask generation process, the proposed method provides better clarity in the outputs compared to the other methods. The proposed hybrid transformation intensifies the skull area (shown in Figure 7, Red rectangles) and CSF area to a great extent. It effectively sharpens the curvature and soft edges in the CSF (shown in Figure-7, Blue rectangles). Additionally, the proposed method highlights tumor areas effectively (shown in Figure 7, Green rectangles).

3.2 Top to Bottom

Original Images, Outputs of S. Karuppanagounder et al.[4], Outputs of AGC[5], Outputs of CLAHE[3], Outputs of Proposed Hybrid method

3.2.1 CT

Regarding the generation of head masks from CT images using the two individual methods discussed above, a slightly different visual observation was made. In some cases, the 'Euclidean distance-based method' failed to completely remove background noise from the CT images (marked with a yellow rectangle in Figure 8). On the other hand, the 'Double-Otsu's threshold method' performed relatively better, but the background noise was not completely eliminated in a few cases (marked with a turquoise blue rectangle in Figure 8).

In Figure 8, the first four rows display five sample images and the outputs of the empirical gamma transformation in[4], adaptive gamma correction[5], and CLAHE[3], respectively. The last two rows show the output of the proposed hybrid method
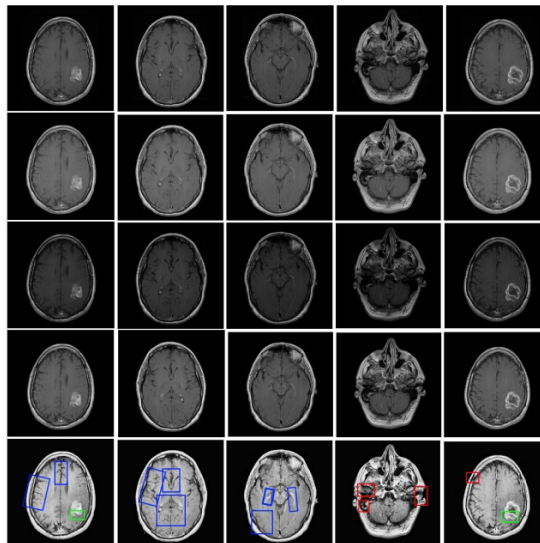
Fig 7. Comparative visual Assessment of MRI images

using the 'Euclidean distance-based mask' and the 'Double-Otsu's threshold method mask'. It is evident from Figure-8 that the proposed method not only enhances contrast but also improves overall brightness in a better way compared to the other methods being compared.
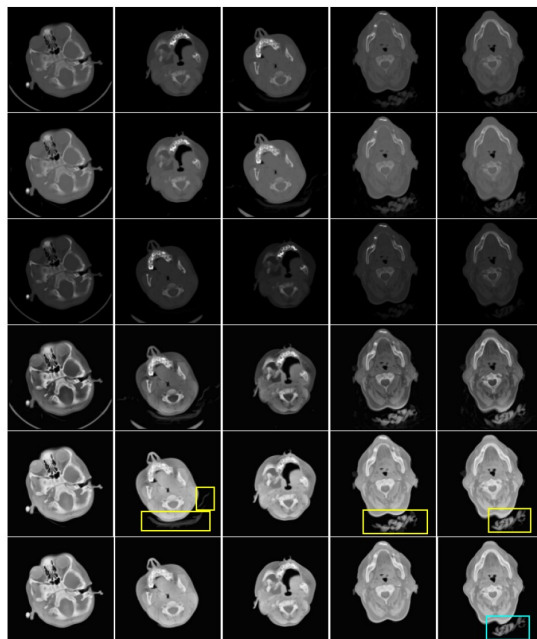

Fig 8. Comparative visual Assesment of CT images

3.3 Top to Bottom

Original Images, Outputs of S. Karuppanagounder et al.[4], Outputs of AGC[5], Outputs of CLAHE[3], Outputs of Proposed Hybrid method (using Euclidean distance masking), Outputs of Proposed Hybrid method (using Double Otsu's Threshold masking)

Quantitative Assessment

Quantitative comparisons have been made regarding Contrast, Entropy, and Correlation[18]. The amount of image enhancement, known as Contrast (CN), has been computed using Equation-13.

$$CN = \frac{1}{MN}\sum_{i=0}^{M-1}\sum_{j=0}^{N-1} I(i,j)^2 - \left(\frac{1}{MN}\sum_{i=0}^{M-1}\sum_{j=0}^{N-1} I(i,j)\right)^2 \tag{13}$$

where, M and N are representing size of the image, and I(i,j) is the pixel intensity.

The amount of information present in the enhanced image, referred to as Entropy (EN), is quantified. The mathematical expression for entropy is given below.

$$EN = \sum_{i=0}^{L-1} n_i * log_2(n_i) \tag{14}$$

where, L is the number of gray levels, and n_i is the probability of a pixel having intensity i.

Spatial correlation (CORR) indicates the linear dependency between specified pairs of pixels. A higher value indicates better enhancement.

$$CORR = \frac{\sum_{i=1}^{M}\left(\sum_{j=1}^{N}\left((i-\mu_x)\cdot(j-\mu_y)\cdot I(i,j)\right\}\right\}}{\sigma_x \times \sigma_y} \tag{15}$$

where, M and N are representing size of the image, I(i,j) is the pixel intensity, μ_x and μ_y are the mean along X and Y direction respectively, σ_x and σ_y are the variance along X and Y direction respectively.

Table 1 presents the average comparative outputs for the 15 MRI and 15 CT-referenced images from the "TCIA"[1] and "Brain CT Images with Intracranial Hemorrhage Masks (BCIIHM)"[12,13] datasets, respectively. The proposed method outperforms the other three methods in all cases. The significant improvement in contrast highlights the novelty of the proposed method, which was the primary objective. Furthermore, the proposed method demonstrates better entropy and intensity correlation compared to the other methods.

On the other hand, Table 2 displays the comparative outputs for 61 MRI and 122 CT images. In the case of MRI, the proposed method outperforms all three methods. However, for the CT dataset, the proposed method ranks second in terms of Contrast and Correlation, but it achieves the best Entropy value among the compared methods.

Table 1. Average comparative study with 15 sample images of TCIA[1] and 15 sample images of "Brain CT Images with Intracranial Hemorrhage Masks (BCIIHM)" datasets[12,13]

Methods	MRI(TCIA)			CT(BCIIHM)		
	Contrast	Correlation	Entropy	Contrast	Correlation	Entropy
Proposed	**0.176267**	**0.984052**	**4.194667**	**0.037892**	**0.995857**	**3.3964**
CLAHE[3]	0.087333	0.975000	3.893333	0.030391	0.991125	3.2792
AGC[5]	0.056000	0.953067	3.886667	0.012364	0.982857	2.7773
EGC[4]	0.075333	0.981200	3.786667	0.018936	0.99343	2.7010

Table 2. Average comparative study with 61 sample images of OASIS dataset[2] and 122 sample images of "Brain metastases" dataset[14]

Methods	MRI(OASIS)			CT (Brain metastases)		
	Contrast	Correlation	Entropy	Contrast	Correlation	Entropy
Proposed	**0.607398**	**0.950696**	**5.927225**	0.165967	0.987026	**3.4798**
CLAHE[3]	0.511493	0.947383	5.819229	**0.178804**	0.985224	3.3775
AGC[5]	0.127291	0.841434	5.393694	0.152909	0.984712	3.2283
EGC[4]	0.207803	0.932974	5.123651	0.11484	**0.98983**	3.0870

This article uses a hybrid methodology that combines the AHE method, local gamma, and global gamma. The 2D-geometric transformation and adaptive gamma algorithms used here use a fuzzy improvement strategy. Through a combination of local and global transformation, a proper balance is maintained to work towards optimal progress. Additionally, the background masking process eliminates the noisy the background pixels, and the augmentation was completed by just taking into account the pixels that make up the head item. On the other hand, AGC[5] and EGC[4] are global techniques, while CLAHE[3] is a local enhancement process. These factors explain why the suggested method outperforms the three earlier methods.

4 Conclusion

This study makes use of a combination of geometric intensity transformation, AHE, and adaptive local and global gamma transformation to boost the contrast of head MRI/CT images. Two distinct background masking techniques, referred to as the "Euclidean distance-based mask" and the "Double-Otsu's threshold method mask," have been introduced to ensure that background pixels are not enhanced. The proposed method does not require for parameter adjustment or training. The results show that the "Double-Otsu's threshold method mask" performs more effectively than the "Euclidean distance-based mask". The proposed method has demonstrated superior performance in enhancing both MRI and CT images compared to the other competing techniques. Quantitatively, for MRI images, the proposed method achieves an average contrast, correlation, and entropy of 0.522319529, 0.957321634, and 5.585280467, respectively. Among the compared methods, CLAHE[3] shows the closest performance to our proposed method, with average values of 0.427776894 for contrast, 0.952833877 for correlation, and 5.439117661 for entropy. In the case of CT images, the proposed method achieves an average contrast, correlation, and entropy of 0.151944190, 0.987992898, and 3.470695978, respectively. Although CLAHE[3] performs slightly better in terms of contrast (0.162554401), it lags behind the proposed method in correlation (0.985870095) and entropy (3.366803956).

These results suggest that the proposed method offers a satisfactory level of contrast enhancement. Although the proposed method surpasses CLAHE[3] in terms of correlation, it does not reach the level of EGC[4] method. It should be emphasized that maintaining a balance among the three parameters (contrast, correlation, and entropy) is essential, and the usability of a method cannot be solely determined by excelling in one parameter while lacking in others. In regard to entropy, the proposed method demonstrates the ability to extract more valuable information from the images, as evidenced by the results compared to the other discussed methods.

In conclusion, the proposed method has proven to be both effective and efficient for enhancing head medical objects. It is important to acknowledge that the scope of the proposed method is limited to the enhancement of head medical objects, and there is potential for future research to explore enhancement techniques for other body components.

References

1) Radhika R, Mahajan R. Medical Image Enhancement: A Review . In: Proceedings of International Conference on Data Science and Applications;vol. 26. Springer Singapore. 2021;p. 105–118.
2) S P, KP B, S B, RK M. Comparative Study on Histogram Equalization Techniques for Medical Image Enhancement [Internet] . *Advances in Intelligent Systems and Computing*. 2019;p. 657– 669. Available from: http://dx.doi.org/10.1007/978-981-15-0035-0_54.
3) Rubini C, Pavithra N. Contrast Enhancementof MRI Images using AHE and CLAHE Techniques. *International Journal of Innovative Technology and Exploring Engineering*. 2019;9(2):2442–2445. Available from: http://dx.doi.org/10.35940/ijitee.B7017.129219.
4) Karuppanagounder S, Palanisamy K. *Medical image contrast enhancement based on gamma correction*. 2011;3:15–18. Available from: https://www.researchgate.net/publication/265352419_Medical_Image_Contrast_Enhancement_based_on_Gamma_Correction.
5) Sahnoun M, Kallel F, Dammak M, Mhiri C, Mahfoudh KB, Hamida AB. A comparative study of MRI contrast enhancement techniques based on Traditional Gamma Correction and Adaptive Gamma Correction: Case of multiple sclerosis pathology. *2018 4th International Conference on Advanced Technologies for Signal and Image Processing (ATSIP)*. 2018. Available from: http://dx.doi.org/10.1109/ATSIP.2018.8364467.
6) Kumar R, Bhandari AK. Spatial mutual information based detail preserving magnetic resonance image enhancement. *Computers in Biology and Medicine*. 2022;146:105644–105644. Available from: http://dx.doi.org/10.1016/j.compbiomed.2022.105644.
7) Arifin AZ, Syuhada F, Ni'mah AT, Suryaningrum DA, Indraswari R, Navastara DA. Teeth Segmentation Using Gamma Adjustment and Transition Region Filter Based on Wavelet Method. *2019 Fourth International Conference on Informatics and Computing (ICIC)*. 2019. Available from: http://dx.doi.org/10.1109/ICIC47613.2019.8985725.
8) Lakshmi AV, Satynarayana V, Mohanaiah DP. MRI Brain Image Enhancement Using an Improved Contrast Enhancement Method. *Revista Gestão Inovação e Tecnologias*. 2021;11(2):607–615. Available from: http://dx.doi.org/10.47059/revistageintec.v11i2.1697.
9) Chen C, Raymond C, Speier W, Jin X, Cloughesy TF, Enzmann DF, et al. Synthesizing MR Image Contrast Enhancement Using 3D High-Resolution ConvNets. *IEEE Transactions on Biomedical Engineering*. 2023;70(2):401–412. Available from: http://dx.doi.org/10.1109/tbme.2022.3192309.
10) Patel P, Cnn-Sice. CNN-SICE Learner Based Image Contrast Enhancement. *International Journal of Applied Science & Engineering*. 2020;8(1). Available from: http://dx.doi.org/10.30954/2322-0465.1.2020.6.
11) Sarkar K, Halder TK, Mandal A. Adaptive power-law and cdf based geometric transformation for low contrast image enhancement. *Multimedia Tools and Applications*. 2021;80(4):6329–6353.
12) Clark K, B V, K S, J F, J K, P K, et al. The Cancer Imaging Archive (TCIA): Maintaining and Operating a Public Information Repository [Internet], 1045–57. Springer Science and Business Media LLC. 2013. Available from: http://dx.doi.org/10.1007/s10278-013-9622-7.
13) Marcus DS, Wang TH, Parker J, Csernansky JG, Morris JC, Buckner RL. Open Access Series of Imaging Studies (OASIS): Cross-sectional MRI Data in Young, Middle Aged, Nondemented, and Demented Older Adults. *Journal Journal of Cognitive Neuroscience*. 2007;19(9):1498 – 1507. Available from: https://doi.org/10.1162/jocn.2007.19.9.1498.
14) M H. Computed Tomography Images for Intracranial Hemorrhage Detection and Segmentation [Internet]. PhysioNet. 2020. Available from: https://physionet.org/content/ct-ich/1.3.1/.
15) Hssayeni MD, Croock MS, Salman AD, Al-Khafaji HF, Yahya ZA, Ghoraani B. Intracranial Hemorrhage Segmentation Using a Deep Convolutional Model. *Data*. 2020;5(1):14–14.
16) Sharma R, Orton T. Brain metastases. 2008. Available from: http://dx.doi.org/10.53347/rid-4924.

17) Q C, L Q, P Y. Performance Analysis of Otsu-Based Thresholding Algorithms: A Comparative Study [Internet]. . *Journal of Sensors*. 2021;2021:1–14. Available from: http://dx.doi.org/10.1155/2021/4896853.

18) Mutlag WK, Ali SK, Aydam ZM, Taher BH. Feature Extraction Methods: A Review. *Journal of Physics: Conference Series*. 2020;1591(1):012028. Available from: http://dx.doi.org/10.1088/1742-6596/1591/1/012028.